

In situ AFM investigation of dual-mode self-assembling peptide

Yue-Xian Bao¹ · Ming Yuan² · Qiqige Du³ · Yu-Bo Li² · Jing-Yu Gao² ·
Abdul Jamil Khan² · Feng Zhang^{1,2,4}

Received: 8 April 2019/Revised: 15 May 2019/Accepted: 23 May 2019/Published online: 10 July 2019

© China Science Publishing & Media Ltd. (Science Press), Shanghai Institute of Applied Physics, the Chinese Academy of Sciences, Chinese Nuclear Society and Springer Nature Singapore Pte Ltd. 2019

Abstract Nanostructures/patterns formed by biomolecules can produce different physicochemical properties in terms of hydrophobicity, zeta-potential, color, etc., which play paramount roles in life. Peptides, as the main bio-building blocks, can form nanostructures with different functions, either in solutions or on interfaces. Previously, we synthesized a short peptide with the inspiration of an Alzheimer's disease-related peptide: amyloid β peptide (A- β), namely GAV-9, which can epitaxially self-assemble into regular nanofilaments on liquid–solid interfaces, and it was found that both the hydrophobicity and charge state of the

interfaces can significantly influence its assembling behavior. It was also reported that another A- β -containing dipeptide, FF, can self-assemble into nanostructures in solutions. Owing to the close relationship between these two short peptides, it is interesting to conjugate them into a de novo peptide with two separated structural domains and study its self-assembling behavior. To this end, herein we have synthesized the GAV-FF peptide with a sequence of $\text{NH}_2\text{-VGGAVVAGVFF-CONH}_2$ and verified its self-assembling property using the in situ liquid-phase atomic force microscopy. The results show that the GAV-FF peptide can self-assemble into nanofilaments both in solutions and on aqueous–solid interfaces, but with different morphologies. The FF domain accelerates the template-assisted self-assembling (TASA) process of the GAV domain, which in return enhances the solubility of FF in aqueous solutions and further participates in the fibrillization of FF. The current results could help deepen the understanding of the aggregation mechanism of disease-related peptides and could also shed light on the strategies to create artificial bio-functional nanostructures/patterns, which hold a significant potential for biomedical applications.

This work was supported by the following programs and foundations: the Program Funded by the University for Fostering Distinguished Young Scholars, the National Natural Science Foundation of China (No. 51763019, U1832125), the China Postdoctoral Science Foundation (No. 2018M630937), the Grassland Talents Program of Inner Mongolia Autonomous Region, the Distinguished Young Scholars Foundation of Inner Mongolia Autonomous Region, and the Young Leading Talents of Science and Technology Program of Inner Mongolia Autonomous Region.

✉ Feng Zhang
fengzhang1978@hotmail.com

¹ College of Animal Science, Inner Mongolia Agricultural University, 306 Zhaowuda Road, Hohhot 010018, China

² Biomedical Nanocenter, School of Life Science, Inner Mongolia Agricultural University, 29 East Erdos Street, Hohhot 010011, China

³ State Key Laboratory of Molecular Engineering of Polymers and Department of Macromolecular Science, Fudan University, 220 Handan Road, Shanghai 200433, China

⁴ Key Laboratory of Oral Medicine, Guangzhou Institute of Oral Disease, Stomatology Hospital, Department of Biomedical Engineering, School of Basic Medical Sciences, Guangzhou Medical University, Guangzhou 511436, China

Keywords Amyloid peptide · Nanofilament · Self-assembly · Structural domain · Atomic force microscopy

1 Introduction

Molecular self-assembly has been considered as a natural technique for constructing functional nanostructures, and the most complex molecular machines, such as enzymes and protein motors, are formed by biomolecule's

self-assembling [1–3]. In general, the main driving force of molecular self-assembly (including folding proteins into three-dimensional structures) normally involves noncovalent interactions such as electrostatic interaction (including the π – π stacking interaction), hydrophobic interaction, and hydrogen-mediated bonding, or the combination of the above-mentioned different interactions. To maintain their stabilities, molecules in aqueous solutions are either charged or neutral. The charge states can be evaluated by the ζ -potential measurement, and some uncharged molecules can still be stable in aqueous solutions owing to the hydrophilic groups conjugated on their surface, such as polyethylene glycol (PEG) and polysaccharides. In life, besides creating useful functional structures, molecular self-assembly can also lead to some disorders such as Alzheimer's disease (AD), Parkinson disease (PD), and other protein aggregation-related diseases [4–6]. Self-assembly is normally concentration dependent, whereby the same molecule with different concentrations can form different morphologic structures, which can be dramatically affected by other conditions such as ionic strength (including pH), temperature, and solvent polarity. Some molecules can not only undergo self-assembly in solutions, but also epitaxially grow into nano-/microstructures on templates, which could be either organic or inorganic substrates. For example, both A- β and α -synuclein (a PD-related protein) can self-assemble into nanofilaments in solutions and on inorganic substrates such as the hydrophilic mica and the hydrophobic graphite [7–9]. In principle, the critical self-assembling concentration (CSC) of molecules on interfaces is much lower than that in solutions, which can be explained by both the space-dimensional confinement effect and the affinity between molecules and templates. With the motivation to reveal the biomolecular self-assembling mechanisms, scientists have been focusing on the self-assembling processes of short protein segments (peptides), and this has already resulted in great advances for deepening the understanding of biological and pathological processes [10].

Atomic force microscopy (AFM) has been accepted as a powerful tool for studying the template-assisted self-assembling (TASA) of biomolecules on different inorganic substrates [9, 11–13]. Because of its easy cleavage and flatness on the millimeter level, mica has become a popular inorganic substrate for AFM imaging. After cleavage, mica normally adsorbs water molecules from the humid air and becomes negatively charged owing to the ionization of potassium ions from the surface, which has been used to mimic the cell membrane in some situations [11, 14, 15]. With liquid-phase AFM and using such substrates, one can observe and record the in situ self-assembly process with a molecular-scale resolution, which until now has not been realized with other high-resolution microscopes, i.e.,

electron microscopy (EM). Using a very soft and sharp tip (normally with a spring constant lower than 1.0 N/m and curvature radius lower than 10 nm), nanostructures can be highly resolved or in situ constructed on the substrates/templates, and the whole construction process can also be dynamically recorded [9, 11, 12]. Nowadays, one can purchase some commercial ultrasharp tips (type: PEAK-FORCE-HIRS-F-B, Bruker Company) with curvature radius of approximately 1.0 nm, which claims to be able to resolve the minor and major grooves of DNA in liquid phase.

Compared to DNA, peptides possess more versatile properties in addition to their self-assembling capability, because the building blocks of peptides, amino acids, not only have more types, but also have more functional groups that can be readily modified and conjugated with other interesting molecules or nanostructures. Therefore, peptides should be the best candidate for creating artificial nanostructures with predesigned functionalities, even though DNA origami has already been developed to a much higher level for constructing nanostructures [16–18]. The other strong evidence is provided by life itself, because life also selects amino acids as the main building blocks for producing bio-nanostructures/machines, which could be also the ultimate goal for scientific researching.

In organisms, long-chain peptides translated from mRNA normally have to experience both intermolecular interactions and intramolecular folding to form bioactivity centers, which are called structural domains in the biological field. In this sense, the folding of peptides could also belong to molecular self-assembly. In this way, the design of dual-functional peptide nanostructures could also be learned from natural biomolecules, so-called bionics. In fact, dual-functional proteins and peptides have been already constructed for different applications [19, 20]. Kang's group, using a bacterial superglue, engineered dual-functional protein cage nanostructures, which act as multiplex fluorescent cell imaging probes that can visualize two or more target cells individually without the need for a set of individual probes [19]. Hamley's group reported a bioactive lipopeptide that combines the capacity to promote the adhesion and subsequent self-detachment of live cells. This peptide, in addition to self-assembling into 3-nm-diameter spherical micelles, can form a coating film that is sensitive to metalloproteases expressed endogenously by the attached cells [20]. Nomizu's group constructed a combined peptide by conjugating a fibronectin active sequence or a scrambled sequence to an amyloid fibril-forming peptide, which can keep their capacities for both fibril formation and cell attachment [21]. Different techniques have also been developed to efficiently screen functional peptides, such as phage display biopanning and split-and-mix library screening based on solid-phase

synthesis. Both techniques make it possible to either study natural peptide systems or create de novo sequences covering a broad spectrum of novel functional molecules and materials [22].

Previously, our research group systematically investigated the self-assembling of a short peptide (GAV-9) on inorganic substrates, such as mica and graphite, which has already attracted significant attention [11, 15]. The interesting part is that the GAV-9 peptide cannot self-assemble into fibrils in pure water solutions (as monitored by thioflavin T (ThT) assay and dynamic light scattering). However, another very short peptide, the FF dipeptide, shows a strong self-assembling capacity in organic solutions but is not soluble in aqueous solutions [23–26]. Therefore, it is a natural idea (also arising from curiosity) to combine these two short peptides together to form a dual-mode assembling peptide, where some interesting questions could be investigated, for example, among the interesting and valuable topics to consider, whether the combined peptide sequence can also show different modes of self-assembling (such as the TASA mode on substrates) and how the competition could be between the hydrophobic and the electrostatic interactions at their different self-assembling modes. Given that the number of biosynthesis systems and possibilities for engineering is nearly infinite, it is wise to restrict the investigation to such a system, which is relatively simple but meaningful with regard to structures and bioactivities [27].

With the aim to construct an artificial peptide with dual self-assembling modes, herein we have synthesized two peptide oligomers called GAV-FF (Fig. 1) and GAV-9, respectively. By using the in situ AFM imaging technique, we have successfully recorded the dynamic TASA process of the GAV-FF peptide on the surface of mica. Further, by comparing the morphologies of the self-assembled GAV-FF nanostructures formed in aqueous solutions and on the

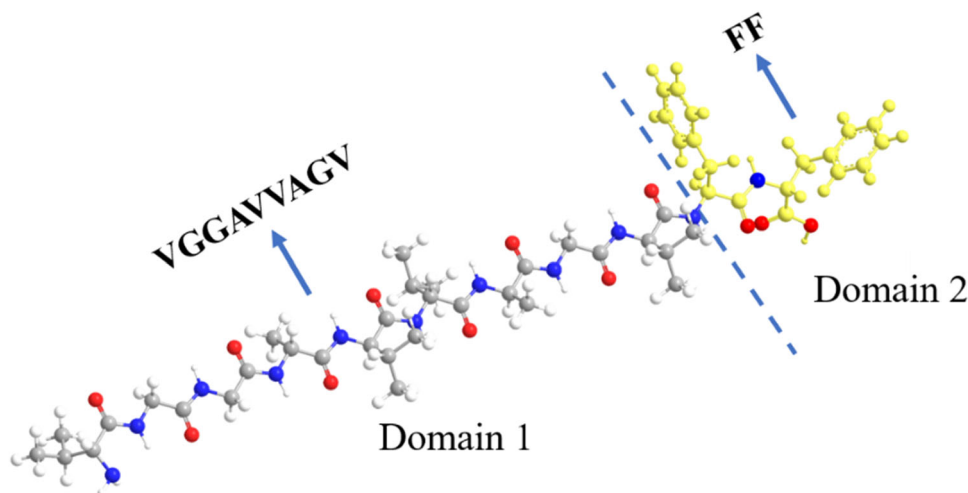
surface of mica, we have proposed different self-assembly modes for the GAV-FF peptide. The obtained results reveal the possibility to produce dual-functional peptides with known capacities by non-genetic means.

2 Experimental section

2.1 Peptide synthesis and preparation

Both GAV-9 ($\text{NH}_2\text{-VGGAVVAGV-CONH}_2$) and GAV-FF ($\text{NH}_2\text{-VGGAVVAGVFF-CONH}_2$) were custom synthesized by a Chinese peptide synthesis company (Taopu Peptide Synthesis Ld. Co.). The carboxylic terminals of both peptides are blocked by acetylation. The peptides were stored at minus 20 °C in a lyophilized powder state, and their purities before use were normally higher than 97%, as verified by both high-performance liquid chromatography (HPLC) and mass spectrum (MS). Due to the difference in peptide solubilities, the stock solutions were prepared as follows: For GAV-FF, 0.5 μg of peptide lyophilized powder was first dissolved in 50 μL of dimethyl sulfoxide (DMSO) and then mixed with 450 μL of Milli-Q water, so that the GAV-FF peptide's concentration was 1.0 mg/mL. For GAV-9, 2.0 mg of peptide powder was dissolved in 1.0 mL of Milli-Q water directly to obtain a concentration of 2.0 mg/mL. The peptide solutions were centrifuged at 10,000 rpm for 10 min to remove any possible aggregates, and they were finally stored in a refrigerator at 4 °C waiting for use. Muscovite mica [$\text{KAl}_2(\text{Si}_3\text{Al})\text{O}_{10}(\text{OH})_2$] was purchased from Sichuan Meifeng Company (China) and freshly cleaved by adhesive tapes to expose a non-contaminated surface before use. All other chemicals, such as DMSO, were purchased from the Sigma-Aldrich Company.

Fig. 1 (Color online) Molecular model and sequence of GAV-FF peptide. The GAV-FF peptide contains two structural domains: One is VGGAVVAGV and the other is FF. G, A, V, and F denote amino acid residues of glycine, alanine, valine, and phenylalanine, respectively



2.2 Atomic force microscopy (AFM)

A commercial AFM (Nanoscope IIIId, Bruker) equipped with either a J-scanner ($125\ \mu\text{m} \times 125\ \mu\text{m}$) or an E-scanner ($12\ \mu\text{m} \times 12\ \mu\text{m}$) was employed to record the whole in situ dynamic process or ex situ nanostructures/patterns of peptide self-assembling on mica surfaces. For the characterization of nanofilaments grown in aqueous solutions, a drop of approximately $2.0\ \mu\text{L}$ of incubated peptide solution was casted on the freshly cleaved mica surface and let it be absorbed for approximately 5 min. Then, it was gently rinsed by Milli-Q water several times, and finally, the sample was dried by compressed air. As for the in situ dynamic observation of TASA on mica, normally a special liquid cell was used, and the holes were all blocked, except for the middle one, for adding peptide solutions with higher concentrations. In brief, approximately $30\ \mu\text{L}$ of Milli-Q water was firstly added into the liquid cell and then started imaging until a stable imaging state was obtained. Then, the highly concentrated peptide solutions were gradually added into the liquid cell dropwise, which somehow is similar to the microtitration reaction operation. During the imaging procedure, the setpoint value was frequently adjusted to keep a minimal force exerted on the samples. The tapping mode was used for both the air and liquid environments, and commercial silicon nitride cantilevers/tips with nominal spring constants, such as smaller than $1\ \text{N/m}$ (SNL-10, Bruker) and larger than $40\ \text{N/m}$, were used for the liquid and air imaging modes, respectively. All the images were captured with a scan rate at $1\text{--}2\ \text{Hz}$ and a resolution of no less than $256\ \text{lines} \times 256\ \text{pixels}$. Using the offline software Nanoscope Analysis version 1.40 (provided by the Bruker Company), all AFM images were processed with the “Flatten” function to remove the tilts during imaging, and both the cross section and growth speed of the peptide nanofilaments could be analyzed.

2.3 Thioflavin T assay

As for the preparation of ThT stock solutions, $0.88\ \text{mg}$ of ThT powder was dissolved in $1.0\ \text{mL}$ of Milli-Q water to obtain a concentration of $1.0\ \mu\text{M}$. For the dynamic monitoring assay of the growth of peptide nanofilaments, a dilution of the ThT stock solution was made by adding $10\ \text{mL}$ of ThT solution ($1\ \mu\text{M}$) into $198\ \text{mL}$ of GAV-FF solution, and they were mixed thoroughly. Then, the mixture solution was added into a 96-well microplate, covered by a piece of sealing film, and placed in the microplate reader (BioTek™ Synergy™ H1 Hybrid Multi-Mode) at $37\ ^\circ\text{C}$ with a vibration frequency of approximately $567\ \text{count per minute (cpm)}$, and the excitation and emission wavelengths were set to $440\ \text{nm}$ and $493\ \text{nm}$,

respectively. The fluorescence intensity was recorded every other 10 min (Fig. 6).

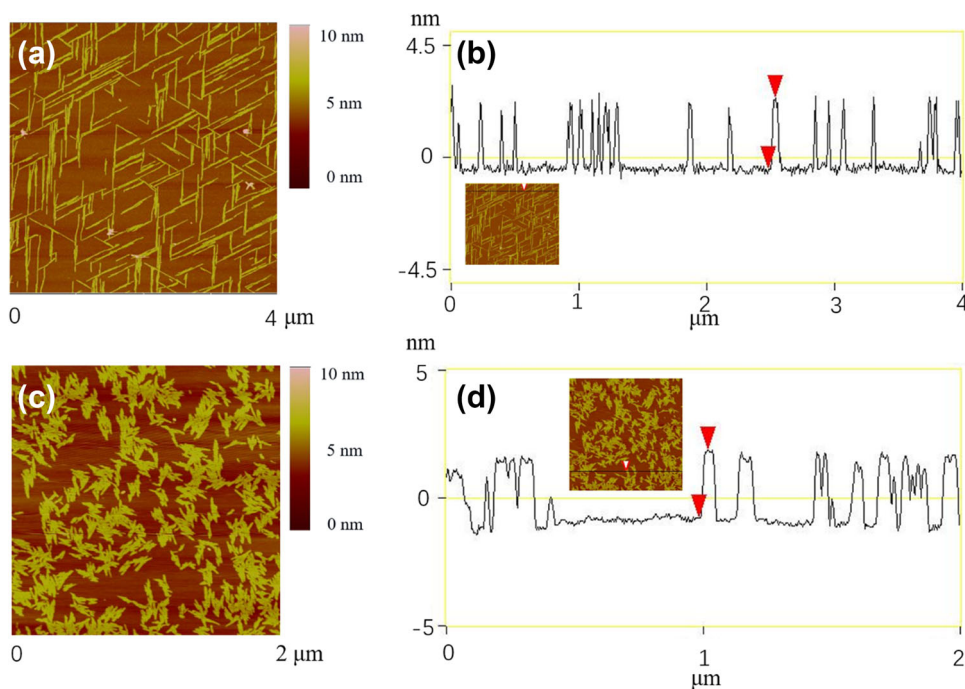
3 Results and discussion

3.1 Design of dual-functional peptide and characterization of its self-assembled nanostructures

Using ex situ AFM, it was found that GAV-FF peptides can form nanofilaments on mica surfaces, but they show different morphologies and growth speeds compared to those of the GAV-9 peptide reported previously [11]. Though GAV-FF grows into membranes/islands with a much higher speed compared to that of GAV-9, the edges of the membrane/island still show three-dimensional preference, indicating that the growth behaviors of both peptides were directed by the atomic lattice of mica, the so-called epitaxial growth. In neutral and basic solutions, the freshly peeled mica surface should be negatively charged and the N-terminal of GAV-9 should be positively charged. Therefore, the electrostatic interaction between the N-terminal of GAV-9 and the mica surface becomes the driving force for the TASA of GAV-9. Figure 2a depicts the morphology of the GAV-9 nanofilaments grown on the surface of mica. It can be seen that the preferred angles between the nanofilaments were 60° , 120° , and 180° , showing triangle, parallel, and quadrilateral shapes from the top view. Because the average center distance of two adjacent amino acid residues is $0.34\ \text{nm}$, the theoretical length of GAV-9 should be $3.06\ \text{nm}$. However, the average height of the GAV-9 nanofilaments is measured as $2.2 \pm 0.1\ \text{nm}$ (Fig. 2b), which is mainly due to dehydration when water is dried in air, and is partially due to the spring constant of the AFM cantilevers used for imaging in air, which is much greater than that used in liquid imaging. From the previous studies, we know that GAV-9 grows into nanofilaments in a “standing up” manner, meaning that GAV-9 molecules adapt a vertical orientation to the mica surface [11].

Figure 2c shows that the morphology of GAV-FF nanofilaments is different from that of GAV-9, and the nanofilaments formed by GAV-FF are much shorter and thicker compared with those of GAV-9, indicating the significant effect on nanofilament morphology with the addition of F residues to the C-terminal of GAV-9. F is a typical aromatic amino acid with a benzene ring. With a diphenylalanine FF modification of GAV-9, the accumulation of $\pi\text{--}\pi$ interactions occurs between the benzene rings of the GAV-FF molecules, which results in stronger intermolecular interaction, namely affinity among peptide molecules. Compared with GAV-9 molecules, the TASA

Fig. 2 (Color online) AFM images and cross-sectional analysis of peptide nanofilaments in air. Morphologic images of nanofilaments formed by GAV-9 (a) and GAV-FF (c), respectively. Cross-sectional analysis of nanofilaments formed by GAV-9 (b) and GAV-FF (d), respectively. All images were taken in air. The cut lines for cross-sectional analysis are indicated by the arrows inside the inset images



of GAV-FF has higher speed, the nanofilament products pile up together quickly, and the growth not only prefers to be one-dimensional, but also shows a fast widening on the lateral directions. In this way, the GAV-FF nanofilaments are shorter and thicker compared to the GAV-9 nanofilaments. As shown in Fig. 2d, the height of the GAV-FF nanofilament is determined to be 2.5 ± 0.1 nm in air, which is about 0.3 nm higher than that of the GAV-9 nanofilaments measured in air. This indicates that the height contribution should come from the addition of FF, and the heights also indicate that both peptides should be still standing up to form nanofilaments on the surface of mica.

FF can self-assemble into nanofilaments in solutions but not on mica surfaces [24], while GAV-9 cannot self-assemble into nanofilaments in aqueous solutions [28] but can epitaxially grow into nanofilaments on mica [11], so it is also interesting to know whether these two different self-assembling capacities/modes could influence each other. Here, by comparing the growth speeds, we found that the addition of FF to the C-terminal of GAV-9 can significantly increase the TASA speed on mica, and in the meanwhile, GAV-FF can also self-assemble into nanofilaments in aqueous solutions, indicating that the addition of GAV-9 to the N-terminal of the FF dipeptide can still maintain its self-assembling capacity. This further proves that the affinity formed by the π - π stacking interaction between aromatic amino acids is much stronger than the hydrophobic interaction between GAV-9 sequences, and we envision that this robust binding could be used for designing other nanostructures.

3.2 Observation of the peptide TASA

The liquid AFM imaging technique allows us to successfully realize in situ observations of the dynamic growth process of peptide nanofilaments on the surface of mica. With this powerful technique, the whole growth of nanofilaments can be recorded from nothing to filaments and to multilayered nanofilament membranes covering the substrates [11, 14]. For the GAV-FF peptide, it was found that the dynamically formed nanofilaments almost cover more than half of the mica surface after 16 min with a concentration of 1.0 mg/mL (Fig. 3), indicating that the growth rate of the nanofilament was much higher than that in GAV-9, with even higher concentration (1.6 mg/mL) as reported previously [11]. In this sense, it can be concluded that the CSC of GAV-FF should be much lower than that of GAV-9 peptide, which can be ascribed to the following two reasons: One is that the solubility of GAV-FF is lower than that of GAV-9, which also increases the hydrophobic interaction among the peptide molecules; the other is that the π - π interaction between FF domains dramatically increases the peptide intermolecular affinity. Due to the rapid growth, especially in the lateral widening directions, the epitaxial growth somehow deviates from the atomic lattice of mica, showing other angles between the nanofilaments after 8 min (Fig. 3d-f). The deviated growth directions could be also affected by the wiping force of the scanning AFM tip. In addition, the rapid growth results in the difficulty to observe single nanofilaments during dynamic in situ imaging, which could be resolved by the

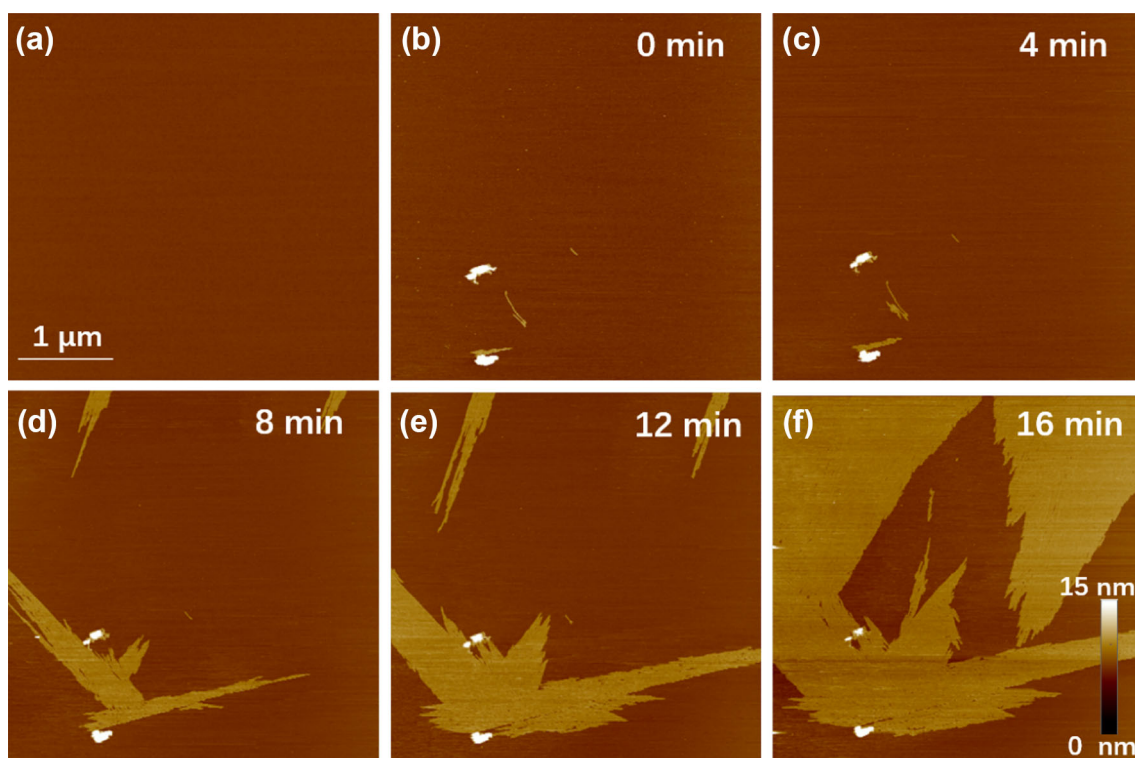


Fig. 3 (Color online) *In situ* observation of the GAV-FF peptide self-assembling procedure. Series snapshots of the self-assembling process of GAV-FF (a–f). The used concentration of GAV-FF was 1.0 mg/

mL. The time taken by the snapshot is shown on the images. Both the horizontal scale and height bars are applied for all images. The AFM tip's scanning direction was horizontal

fast scanning function of some novel models of AFM in the future.

The cross-sectional analysis shows that the average height of the GAV-FF filaments obtained in the solutions is 3.2 ± 0.1 nm (Fig. 4a, b), which is approximately 0.6 nm higher than the nanofilaments formed by GAV-9 in pure water on mica (data not shown). Owing to the smaller force that AFM exerts under tapping mode on the nanofilaments during the liquid imaging process, the height of nanofilaments is not compressed; therefore, it can reflect the true height compared with those obtained for the AFM images

recorded in air. In addition, the peptide might be more outstretched in solutions than in a dried state, such as in air. Because the single nanofilaments were difficult to resolve with the current AFM system, the growth speed is shown by plotting the covering area against growth time. From this, we can deduce that the nanofilament growth involves a positive cooperativity, in which the plot curve shows an exponential growth model (Fig. 4c), and this phenomenon further proves that the formed nanofilaments might act as “seeds” to accelerate the growth of new nanofilaments. The lateral widening of nanofilaments due to the increased

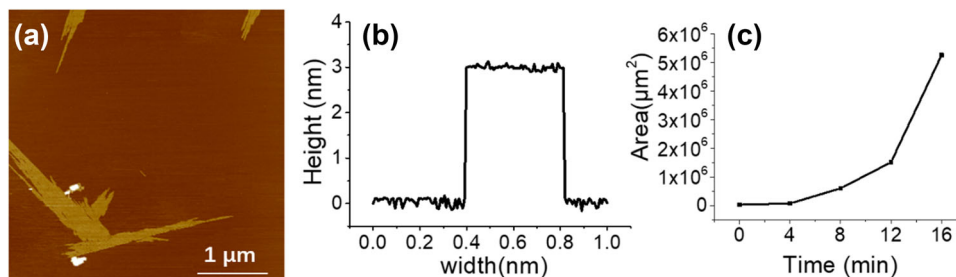


Fig. 4 Height and growth speed analysis of GAV-FF peptide nanofilaments. **a** One AFM height mode image obtained from the *in situ* imaging process conducted in water. **b** Cross-sectional analysis of the GAV-FF nanofilaments obtained from the AFM height mode image from (a). The height is measured to be 3.2 ± 0.1 nm. Because the height analysis is conducted for many nanofilaments grown

adjacently in parallel, the measured value can reflect an average height of the GAV-FF nanofilaments. **c** Growth curve of GAV-FF nanofilaments obtained by plotting the covering area of the nanofilaments on the surface of mica against the observation time. The covering area of the nanofilaments was obtained by using the ImageJ analysis software

intermolecular interactions could account for the positive cooperativity of the GAV-FF nanofilament growth on mica, in which the more the peptide molecules participate into the nanofilaments, the more the periphery interacting interface is exposed around the nanofilaments. Then, more GAV-FF can be attracted to join in the formation of nanofilaments, which in return drives the TASA process positively.

3.3 Characterization and kinetics of GAV-FF nanofilaments formed in solutions

To verify the fibrillization capacity of the GAV-FF peptide in aqueous solutions, GAV-FF peptide solutions were prepared and incubated at room temperature without agitation for 24 h. Further, to avoid the TASA influence, the samples were diluted at least three times before being casted on the freshly cleaved mica surface, and the absorption time was also limited within 5 min with the aim to avoid the rise in concentration due to water evaporation. As a result, it was found that GAV-FF formed a large number of nanofilaments in aqueous solutions (Fig. 5), indicating that the FF structural domain maintains its self-assembling capacity even after conjugating with the GAV structural domain. This phenomenon tells us that the short nanofilament-forming peptide can attract other interesting molecules into its nanostructures. This has actually been used for vaccine design and has already been demonstrated by several groups [29–33]. Because of the strong interaction of the FF structural domain, GAV-FF peptides were brought together to form one-dimensional nanofilaments in solutions. In this sense, the addition of the FF structural domain also affects the self-assembling nature of the GAV-9 peptide. Figure 5 shows that the nanofilament heights are not homogenous, and the measured heights are mainly distributed between 1.0 nm and 3.0 nm, indicating a hierarchical self-assembling mode involved in the formation of GAV-FF nanofilaments.

In general, the uneven nanofilaments formed by peptides or proteins could be cataloged into two classes of hierarchical self-assembling: In one case, the molecular building blocks firstly form the basic one-dimensional nanofilament/ protofilaments, and then these nanofilaments can twist together to further form thicker nanofilaments with periodic peaks and valleys along their growth axis [34]. In the other case, the process extends from monomers to oligomers and final assemble into nanofilaments [35]. These two self-assembling modes share common morphologies such as the coexistence of both types of nanofilaments with different diameters and the periodic peaks and valleys along the growth axis of nanofilaments. These two types of self-assembling modes can be distinguished by considering whether the periodicity along the growth axis changes as

the nanofilament diameter changes. This is because the second mode normally maintains the periodicity, while the first mode changes significantly. In our case, the horizontal distances between the adjacent peaks or valleys along the growth axis of the nanofilaments were differentiated by approximately 10.8 ± 0.1 nm among nanofilaments with a vertical peak-to-valley difference of approximately 0.2 nm (Fig. 5). In combination with the above-mentioned self-assembling modes, we conclude that the current self-assembling mode should belong to the first case in that the hierarchical self-assembling exhibits different periodicities along the fast growth axis of the nanofilaments.

To study the dynamic fibrillization process of GAV-FF in solutions, the ThT assay was employed. As is known, ThT is a β -sheet-specific molecular probe, which changes its fluorescence quantum yield upon binding/inserting to β -sheet structures, and ThT has been successfully used to quantify the amyloid fibril structure mainly for amyloidogenesis [36–38]. As reported by Takeda's group, the fluorescence change of ThT can be linear from 0 to 2.0 $\mu\text{g/mL}$ amyloid fibrils [36]. Since its first description in 1959, the ThT assay has become the most widely used “gold standard” for selectively staining and identifying amyloid fibrils both in vivo and in vitro [39]. Until now, scientists have discovered the principle of ThT fluorescence upon binding β -sheet structures, in which the rotation of the benzene ring of ThT will be confined/restricted as they insert into the lamella of β -sheet structures, resulting in the mechanical energy transferring to radiation energy, fluorescence. This has been called aggregation-induced emission (AIE) [40].

In practice, the maximum emission at 493 nm can be dramatically increased as ThT binds to β -sheet structures with an optimized excitation wavelength at 440 nm. In the current study, the fluorescence signal gradually rises as the GAV-FF solution was incubated at room temperature within 4 h (Fig. 6). In contrast, the fluorescence intensity of pure ThT did not change within this period, which verifies the feasibility of the ThT assay for quantification of GAV-FF nanofilaments. After 50 min of incubation, the fluorescence intensity reached its plateau, in which the fluorescence intensity remained unchanged, indicating that the nanofilaments reached the growth equilibrium. The rapid fibrillization speed further proves the strong affinity between GAV-FF peptides in solutions. Meanwhile, the dramatic fluorescence change also indicates that the major components of the nanofilaments should be β -sheets as they can be specifically bonded by ThT.

3.4 Molecular mechanism of GAV-FF fibrillization

In comparison with the nanofilaments formed both on mica surfaces and in solutions, one can clearly consider that the different self-assembling modes should account for

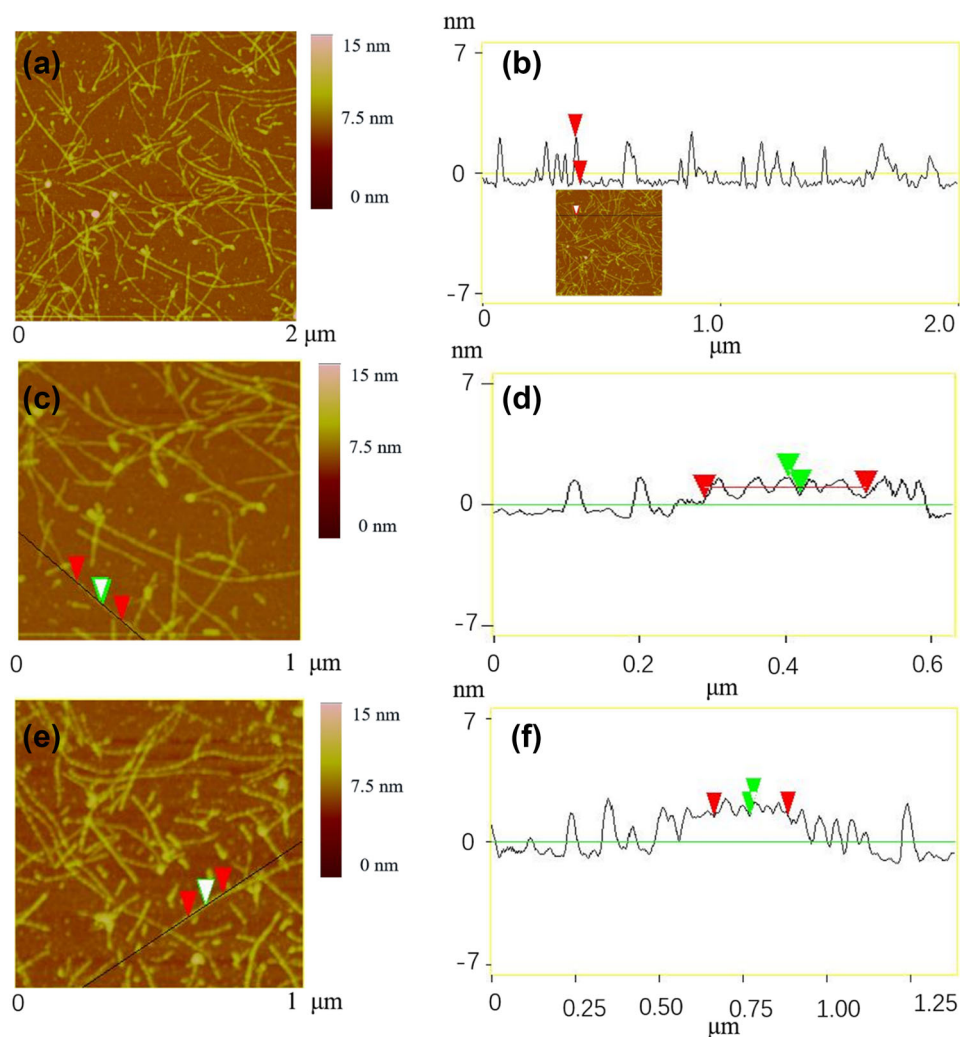


Fig. 5 (Color online) AFM characterization of GAV-FF nanofilaments formed in solutions. **a** AFM height mode image of GAV-FF nanofilaments formed in solutions. **b** Cross-sectional analysis of nanofilaments of GAV-FF formed in solutions. The black line in the inset image denotes the cut line for the cross-sectional analysis, and the height between two red marks indicates the diameter of the measured GAV-FF nanofilament, 2.9 ± 0.1 nm. As for the longitudinal periodicity analysis of the GAV-FF nanofilaments formed in solutions, AFM height mode images of GAV-FF nanofilaments

formed in solutions are shown in **(c)** and **(e)**. The longitudinal cross-sectional analysis of GAV-FF nanofilaments with different diameters is shown in **(d)** and **(f)**. The black lines in **(c)** and **(e)** denote the cutting lines for the longitudinal cross-sectional analysis, and the colored arrows denote the measurements for both height (green colored) and length (red colored). The average periodicities of the nanofilaments are approximately 44.3 nm in **(c)** and 33.5 nm in **(e)**, respectively. The average peak-to-valley heights are approximately 0.9 nm and 0.7 nm, as denoted in **(d)** and **(f)**, respectively

the formation of nanofilaments. On the surface of mica, it is apparent that peptides adopt the TASA mode, in which the fast growth axis of the nanofilaments exhibits three preferred orientations despite being confined inside the two-dimensional plane. Moreover, owing to the positive cooperative effect driven by the strong π - π interactions between FF structural domains, the lateral widening speed of nanofilaments significantly increased compared to that of the GAV-9 peptide, which results in the rapid formation of an island-like monolayer, although its edges show small deviations to the regular triangles as formed by GAV-9 peptide. In combination of the homogenous height and the three preferred fast growth orientations, we propose that

the GAV-FF peptide maintains the epitaxial growth manner (Fig. 7a) as the GAV-9 peptide does [11]. While in solutions, the GAV-FF peptide forms freestanding nanofilaments with periodical peaks and valleys distributed along the fast growth axis of the nanofilaments. According to statistics, different nanofilaments show different periodical distances between the adjacent peaks or valleys, which resembles one typical hierarchical self-assembling mode: The peptides first form single nanofilaments and then further twist into hemp cord-like one-dimensional nanostructures (Fig. 7b).

As can be seen, the different regions of the same nanofilament show different heights (Fig. 5a, b), and the

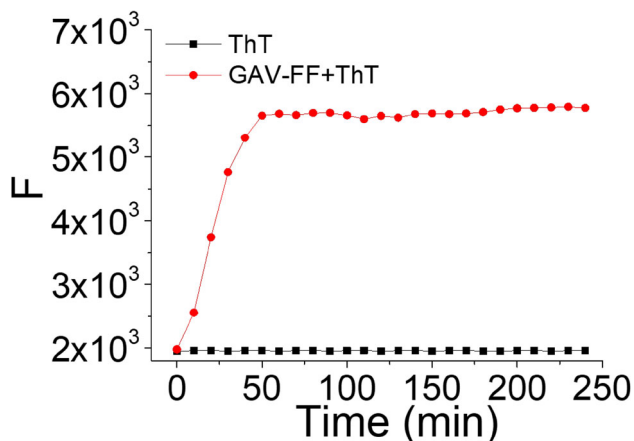


Fig. 6 ThT assay of GAV-FF nanofilaments formed in solutions. The curves were obtained by plotting the fluorescence intensity (F) against the incubation time (min). A control experiment, denoted by ThT only, was conducted with the same condition. All the data were collected from a 96-well microplate reader at 37 °C under vibration conditions. The excitation and emission wavelengths were set to 440 nm and 493 nm, respectively

periodicities of different nanofilaments are not regular (Fig. 5c–f). By cross-sectional analysis of the nanofilament heights, we found that the biggest height was measured to

approximately 2.7 ± 0.1 nm, which is even less than the height of GAV-FF nanofilaments formed on mica surface. On the one hand, the dehydration of nanofilaments may reduce their diameter, and on the other hand, the AFM images obtained in air could also reduce the real diameter of nanofilaments. In addition, it might be complicated than the schematic illustration of nanofilaments as shown in Fig. 7b. However, we believe that the FF structural domains provide the driving force and they should firstly bind together to form the lowest/simplest level of nanofilaments, which further twist together to form higher hierarchical nanofilaments. By measuring the longitudinal periodicity of a single nanofilament, we obtain that the difference between the peak and valley of the thinner nanofilament is approximately 0.9 nm, and the distance between two adjacent peaks is 44.3 nm. However, the difference between the peak and the valley of the thicker nanofilament is of approximately 0.7 nm and the distance between two adjacent peaks is 33.4 nm. We speculate that the larger the periodicity exhibited along the fast growth axis of the nanofilaments, the more the protofilaments twist together.

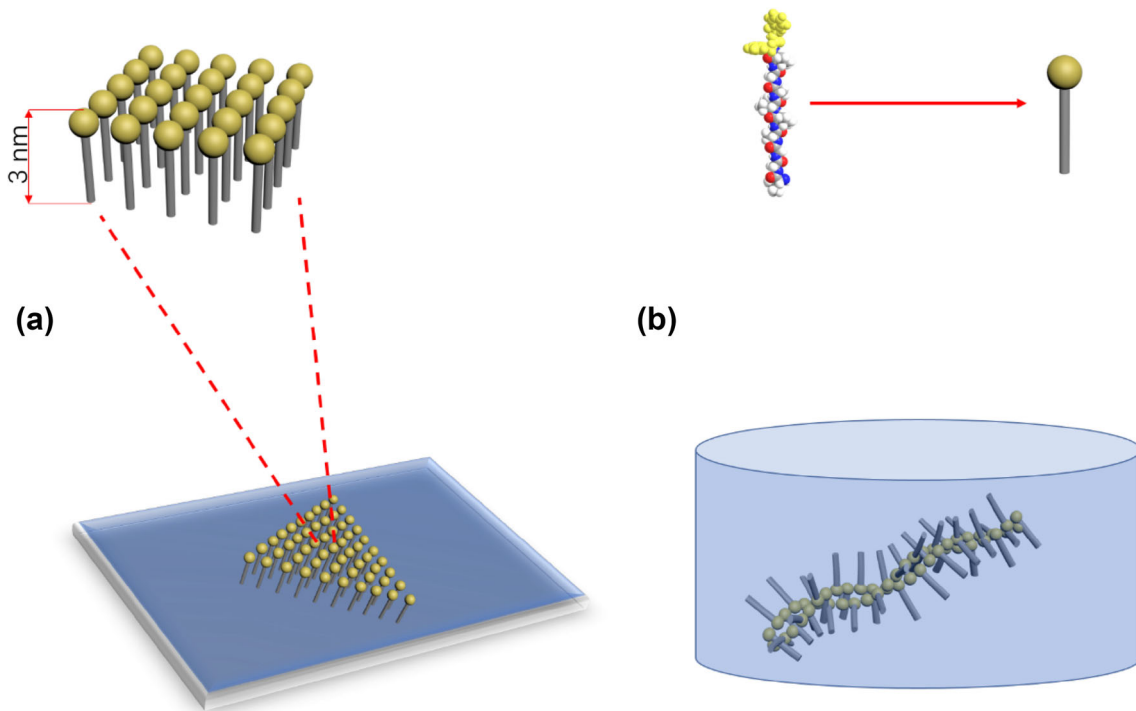


Fig. 7 (Color online) Schematic illustration of GAV-FF nanostructures formed on mica and in aqueous solutions. The GAV-FF peptide is simplified to a stick with a head, in which yellow balls represent the FF structural domains, and gray sticks represent the GAV-9 sequence. **a** Self-assembling mode of GAV-FF peptide on mica: The nanofilaments form triangle-like islands on mica, and the peptides adopt a

“standing up” manner to form nanofilaments with a homogenous height which is equal to the theoretical length of the GAV-FF peptide (~ 3.2 nm). **b** Possible nanofilaments formed by two twisting protofilaments (the simplest nanostructures) formed by GAV-FF peptide in solutions

4 Conclusion

Multifunctional nanostructures are an active area of scientific research. With the aim to demonstrate a novel idea, we have constructed and synthesized a de novo designed peptide oligomer just by combining two self-assembling short peptides together. By making best use of the in situ liquid AFM imaging technique, the self-assembled nanofilaments formed both on the surface of mica and in the aqueous solutions have been thoroughly characterized and analyzed. It is found that both structural domains can carry out their own functionalities, meaning that the novel GAV-FF peptide not only can grow epitaxially into nanofilaments on the surface of mica, but also can self-assemble into freestanding nanofilaments in aqueous solutions, indicating that both structural domains maintain their own functionalities. With the comprehensive analysis of the morphologies and kinetics of GAV-FF nanofilaments, we have proposed the possible self-assembling mechanisms for the nanofilaments formed both on the surface of mica and in aqueous solutions. In brief, the GAV-FF peptide adopts the TASA mode and stands up in lines to form nanofilaments on the surface of mica, in which the GAV-9 structural domain plays a dominant role, and the FF domain enhances the intermolecular interactions and exhibits a more rapid speed of TASA. While in solutions, the FF structural domain plays the dominant role to fibrillate into freestanding protofilaments, which further twist into hemp cord-like nanofilaments with variable periodicities. The kinetics of the GAV-FF self-assembling has been also studied by using ThT assays, and the results show a typical sigmoidal growth curve. Meanwhile, this indicates that the nanofilaments formed in solutions should consist of β -sheet structures. In combination with all these results, we have proposed a hierarchical self-assembling mode for GAV-FF peptide in solutions. The results of this research are helpful to better understand the aggregation mechanism of disease-related peptides and also could shed light on strategies for constructing functional nanostructures of artificial organisms, which holds great potential for biomedical applications.

References

1. R. Zhong, Q. Tang, S. Wang et al., Self-assembly of enzyme-like nanofibrous G-molecular hydrogel for printed flexible electrochemical sensors. *Adv. Mater.* **30**, 1706887 (2018). <https://doi.org/10.1002/adma.201706887>
2. Y. Zhao, W. Yang, C. Chen et al., Rational design and self-assembly of short amphiphilic peptides and applications. *Curr. Opin. Colloid Interface Sci.* **35**, 112–123 (2018). <https://doi.org/10.1016/j.cocis.2018.02.009>
3. Y. Liu, Self-assembly: supramolecular basketry. *Nat. Chem.* **9**, 1037–1038 (2017). <https://doi.org/10.1038/nchem.2883>
4. F. Rousseau, J. Schymkowitz, L. Serrano, Protein aggregation and amyloidosis: confusion of the kinds? *Curr. Opin. Struct. Biol.* **16**, 118–126 (2006). <https://doi.org/10.1016/j.sbi.2006.01.011>
5. P.T. Lansbury, H.A. Lashuel, A century-old debate on protein aggregation and neurodegeneration enters the clinic. *Nature* **443**, 774–779 (2006). <https://doi.org/10.1038/nature05290>
6. A. Aguzzi, T. O'Connor, Protein aggregation diseases: pathogenicity and therapeutic perspectives. *Nat. Rev. Drug Discov.* **9**, 237–248 (2010). <https://doi.org/10.1038/nrd3050>
7. G. Yang, K.A. Woodhouse, C.M. Yip, Substrate-facilitated assembly of elastin-like peptides: studies by variable-temperature in situ atomic force microscopy. *J. Am. Chem. Soc.* **124**, 10648–10649 (2002). <https://doi.org/10.1021/ja027302g>
8. C. Whitehouse, J.Y. Fang, A. Aggeli et al., Adsorption and self-assembly of peptides on mica substrates. *Angew. Chem. Int. Ed.* **44**, 1965–1968 (2005). <https://doi.org/10.1002/anie.200462160>
9. T. Kowalewski, D.M. Holtzman, In situ atomic force microscopy study of Alzheimer's beta-amyloid peptide on different substrates: new insights into mechanism of beta-sheet formation. *Proc. Natl. Acad. Sci. USA* **30**, 3688–3693 (1999). <https://doi.org/10.1073/pnas.96.7.3688>
10. M. Amit, S. Yuran, E. Gazit et al., Tailor-made functional peptide self-assembling nanostructures. *Adv. Mater.* **30**, 1707083 (2018). <https://doi.org/10.1002/adma.201707083>
11. F. Zhang, H.N. Du, Z.X. Zhang et al., Epitaxial growth of peptide nanofilaments on inorganic surfaces: effects of interfacial hydrophobicity/hydrophilicity. *Angew. Chem. Int. Ed. Engl.* **45**, 3611–3613 (2006). <https://doi.org/10.1002/anie.200503636>
12. X. Liu, Y. Zhang, D.K. Goswami et al., The controlled evolution of a polymer single crystal. *Science* **307**, 1763–1766 (2005). <https://doi.org/10.1126/science.1109487>
13. M.S. Kellermayer, A. Karsai, M. Benke et al., Stepwise dynamics of epitaxially growing single amyloid fibrils. *Proc. Natl. Acad. Sci. USA* **105**, 141–144 (2008). <https://doi.org/10.1073/pnas.0704305105>
14. Q. Du, B. Dai, J. Hou et al., A comparative study on the self-assembly of an amyloid-like peptide at water-solid interfaces and in bulk solutions. *Microsc. Res. Techniq.* **78**, 375–381 (2015). <https://doi.org/10.1002/jemt.22483>
15. J.H. Hou, Q.Q.G. Du, R.B. Zhong et al., Temperature manipulating peptide self-assembly in water nanofilm. *Nucl. Sci. Tech.* **25**, 060502 (2014). <https://doi.org/10.13538/j.1001-8042/nst.25.060502>
16. D. Han, S. Pal, J. Nangreave et al., DNA origami with complex curvatures in three-dimensional space. *Science* **332**, 342–346 (2011). <https://doi.org/10.1126/science.1202998>
17. M.S. Strano, Functional DNA origami devices. *Science* **338**, 890–891 (2012). <https://doi.org/10.1126/science.1231024>
18. K. Sanderson, Bioengineering: what to make with DNA origami. *Nature* **464**, 158–159 (2010). <https://doi.org/10.1038/464158a>
19. Y. Bae, G.J. Kim, H. Kim et al., Engineering tunable dual functional protein cage nanoparticles using bacterial superglue. *Biomacromolecules* **19**, 2896–2904 (2018). <https://doi.org/10.1021/acs.biomac.8b00457>
20. A. Dehsorkhi, R.M. Gouveia, A.M. Smith et al., Self-assembly of a dual functional bioactive peptide amphiphile incorporating both matrix metalloprotease substrate and cell adhesion motifs. *Soft Matter* **11**, 3115–3124 (2015). <https://doi.org/10.1039/c5sm00459d>
21. S. Kasai, Y. Ohga, M. Mochizuki et al., Multifunctional peptide fibrils for biomedical materials. *Biopolymers* **76**, 27–33 (2004). <https://doi.org/10.1002/bip.10565>
22. N. Ten Brummelhuis, P. Wilke, H.G. Borner, Identification of functional peptide sequences to lead the design of precision

- polymers. *Macromol. Rapid Commun.* **38**, 1700632 (2017). <https://doi.org/10.1002/marc.201700632>
23. G. Singh, A.M. Bittner, S. Loscher et al., Electrospinning of diphenylalanine nanotubes. *Adv. Mater.* **20**, 2332–2336 (2008). <https://doi.org/10.1002/adma.200702802>
 24. X.H. Yan, P.L. Zhu, J.B. Li, Self-assembly and application of diphenylalanine-based nanostructures. *Chem. Soc. Rev.* **39**, 1877–1890 (2010). <https://doi.org/10.1039/b915765b>
 25. J. Kim, T.H. Han, Y.I. Kim et al., Role of water in directing diphenylalanine assembly into nanotubes and nanowires. *Adv. Mater.* **22**, 583–587 (2010). <https://doi.org/10.1002/adma.200901973>
 26. J. Ryu, C.B. Park, Synthesis of diphenylalanine/polyaniline core/shell conducting nanowires by peptide self-assembly. *Angew. Chem. Int. Ed.* **48**, 4820–4823 (2009). <https://doi.org/10.1002/anie.200900668>
 27. T. Dang, R.D. Sussmuth, Bioactive peptide natural products as lead structures for medicinal use. *Acc. Chem. Res.* **50**, 1566–1576 (2017). <https://doi.org/10.1021/acs.accounts.7b00159>
 28. H. Li, F. Zhang, Y. Zhang et al., Organic solvents mediate self-assembly of GAV-9 peptide on mica surface. *Acta Biochim. Biophys. Sin.* **39**, 285–289 (2007). <https://doi.org/10.1111/j.1745-7270.2007.00278.x>
 29. A.W. Purcell, J. McCluskey, J. Rossjohn, More than one reason to rethink the use of peptides in vaccine design. *Nat. Rev. Drug Discov.* **6**, 404–414 (2007). <https://doi.org/10.1038/nrd2224>
 30. P. Burkhard, J. Stetefeld, S.V. Strelkov et al., Coiled coils: a highly versatile protein folding motif. *Trends Cell Biol.* **11**, 82–88 (2001). [https://doi.org/10.1016/s0962-8924\(00\)01898-5](https://doi.org/10.1016/s0962-8924(00)01898-5)
 31. J.S. Rudra, Y.F. Tian, J.P. Jung et al., A self-assembling peptide acting as an immune adjuvant. *Proc. Natl. Acad. Sci. USA* **107**, 622–627 (2010). <https://doi.org/10.1073/pnas.0912124107>
 32. G.A. Hudalla, T. Sun, J.Z. Gasiorowski et al., Graded assembly of multiple proteins into supramolecular nanomaterials. *Nat. Mater.* **13**, 829–836 (2014). <https://doi.org/10.1038/nmat3998>
 33. G.A. Hudalla, J.A. Modica, Y.F. Tian et al., A self-adjuvanting supramolecular vaccine carrying a folded protein antigen. *Adv. Healthc. Mater.* **2**, 1114–1119 (2013). <https://doi.org/10.1002/adhm.201200435>
 34. N.M. Kad, S.L. Myers, D.P. Smith et al., Hierarchical assembly of beta2-microglobulin amyloid in vitro revealed by atomic force microscopy. *J. Mol. Biol.* **330**, 785–797 (2003). [https://doi.org/10.1016/S0022-2836\(03\)00583-7](https://doi.org/10.1016/S0022-2836(03)00583-7)
 35. E. Gazit, Self assembly of short aromatic peptides into amyloid fibrils and related nanostructures. *Prion* **1**, 32–35 (2007). <https://doi.org/10.4161/pri.1.1.4095>
 36. H. Naiki, K. Higuchi, M. Hosokawa et al., Fluorometric determination of amyloid fibrils in vitro using the fluorescent dye, thioflavine T. *Anal. Biochem.* **2**, 244–249 (1989). [https://doi.org/10.1016/0003-2697\(89\)90046-8](https://doi.org/10.1016/0003-2697(89)90046-8)
 37. H. LeVine III, Thioflavine T interaction with synthetic Alzheimer's disease beta-amyloid peptides: detection of amyloid aggregation in solution. *Protein Sci.* **3**, 404–410 (1993). <https://doi.org/10.1002/pro.5560020312>
 38. R. Khurana, C. Coleman, C. Ionescu-Zanetti et al., Mechanism of thioflavin T binding to amyloid fibrils. *J. Struct. Biol.* **3**, 229–238 (2005). <https://doi.org/10.1016/j.jsb.2005.06.006>
 39. P.S. Vassar, C.F. Culling, Fluorescent stains, with special reference to amyloid and connective tissues. *Arch. Pathol.* **68**, 487–498 (1959)
 40. G. Feng, B. Liu, Aggregation-induced emission (AIE) dots: emerging theranostic nanolights. *Acc. Chem. Res.* **51**, 1404–1414 (2018). <https://doi.org/10.1021/acs.accounts.8b00060>